EVOLUTION

Cross-Species Protein Interactome Mapping Reveals Species-Specific Wiring of Stress Response Pathways

Jishnu Das,[1,2]* Tommy V. Vo,[2,3]* Xiaomu Wei,[2,4] Joseph C. Mellor,[5] Virginia Tong,[2] Andrew G. Degatano,[2] Xiujuan Wang,[1,2] Lihua Wang,[2] Nicolas A. Cordero,[2] Nathan Kruer-Zerhusen,[2,3] Akihisa Matsuyama,[6,7] Jeffrey A. Pleiss,[3] Steven M. Lipkin,[4] Minoru Yoshida,[6,7,8] Frederick P. Roth,[5,9,10,11,12,13] Haiyuan Yu[1,2]†

The fission yeast *Schizosaccharomyces pombe* has more metazoan-like features than the budding yeast *Saccharomyces cerevisiae*, yet it has similarly facile genetics. We present a large-scale verified binary protein-protein interactome network, "StressNet," based on high-throughput yeast two-hybrid screens of interacting proteins classified as part of stress response and signal transduction pathways in *S. pombe*. We performed systematic, cross-species interactome mapping using StressNet and a protein interactome network of orthologous proteins in *S. cerevisiae*. With cross-species comparative network studies, we detected a previously unidentified component (Snr1) of the *S. pombe* mitogen-activated protein kinase Sty1 pathway. Coimmunoprecipitation experiments showed that Snr1 interacted with Sty1 and that deletion of *snr1* increased the sensitivity of *S. pombe* cells to stress. Comparison of StressNet with the interactome network of orthologous proteins in *S. cerevisiae* showed that most of the interactions among these stress response and signaling proteins are not conserved between species but are "rewired"; orthologous proteins have different binding partners in both species. In particular, transient interactions connecting proteins in different functional modules were more likely to be rewired than conserved. By directly testing interactions between proteins in one yeast species and their corresponding binding partners in the other yeast species with yeast two-hybrid assays, we found that about half of the interactions that are traditionally considered "conserved" form modified interaction interfaces that may potentially accommodate novel functions.

INTRODUCTION

A crucial step toward understanding the properties of cellular systems is to map networks of DNA-protein, RNA-protein, and protein-protein interactions, or the "interactome network," of an organism. Over the last decade, large-scale binary protein-protein interactome data sets have been produced for several eukaryotes—*Saccharomyces cerevisiae* (*1*–*3*), *Drosophila melanogaster* (*4*, *5*), *Caenorhabditis elegans* (*6*, *7*), *Arabidopsis thaliana* (*8*), and human (*9*, *10*), among which we produced a high-quality whole-proteome interactome network in *S. cerevisiae* using a high-throughput yeast two-hybrid (HT-Y2H) system (*1*). However, because of large evolutionary distances among these species [the last common ancestor of fungi and human is over 1 billion years ago (*11*, *12*)] and extremely low coverage (most protein interactions are yet to be detected) of available interactome maps outside of *S. cerevisiae*, the overlap among these networks is sparse (*13*). This makes it difficult to extract meaningful information about evolutionary relationships from these interactomes. Thus, to bridge this gap, it is essential to construct a high-coverage interactome network for an intermediate species. The fission yeast *Schizosaccharomyces pombe* has an easily manipulatable genome and is estimated to have diverged from the budding yeast *S. cerevisiae* about 400 million years ago (*11*, *12*). Furthermore, fission yeast is more similar to metazoans than is budding yeast, especially in its gene regulation by chromatin modification and RNA interference, mechanisms that are differently regulated and absent, respectively, in budding yeast (*14*). A high-quality map of the protein-protein interactome network of *S. pombe* will enable analysis of the biological properties of many complex pathways common in metazoan species but missing in *S. cerevisiae* (*15*).

The two yeast species live in highly disparate ecological niches and have varied mechanisms of responding to external stimuli. Therefore, in this study, we focus on 658 *S. pombe* genes involved in key regulatory processes of stress response and cellular signaling. Because these pathways control how organisms sense and adapt to their immediate environments, they are likely to have diverged between the two species. Using our HT-Y2H pipeline (*1*), we obtained a binary interactome network among these 658 genes, which we named "StressNet." All interactions were verified with two orthogonal assays to ensure their quality. By comparing with their *S. cerevisiae* counterparts, we measured the conservation rate of these StressNet interactions between fission and budding yeast using

[1]Department of Biological Statistics and Computational Biology, Cornell University, Ithaca, NY 14853, USA. [2]Weill Institute for Cell and Molecular Biology, Cornell University, Ithaca, NY 14853, USA. [3]Department of Molecular Biology and Genetics, Cornell University, Ithaca, NY 14853, USA. [4]Department of Medicine, Weill Cornell College of Medicine, New York, NY 10021, USA. [5]Donnelly Centre, University of Toronto, Toronto, Ontario M5S 3E1, Canada. [6]Chemical Genetics Laboratory, RIKEN Advanced Science Institute, Wako, Saitama 351-0198, Japan. [7]CREST Research Project, JST, Kawaguchi, Saitama 332-0012, Japan. [8]Department of Biotechnology, Graduate School of Agriculture and Life Sciences, University of Tokyo, Bunkyo-ku, Tokyo 113-8657, Japan. [9]Departments of Molecular Genetics and Computer Science, University of Toronto, Toronto, Ontario M5S 3E1, Canada. [10]Center for Cancer Systems Biology, Dana-Farber Cancer Institute, Boston, MA 02115, USA. [11]Harvard Medical School, Boston, MA 02115, USA. [12]Samuel Lunenfeld Research Institute, Mt. Sinai Hospital, Toronto, Ontario M5G 1X5, Canada. [13]Genetic Networks Program, Canadian Institute for Advanced Research, Toronto, Ontario M5G 1Z8, Canada.
*These authors contributed equally to this work.
†Corresponding author. E-mail: haiyuan.yu@cornell.edu

a Bayesian method. We found species-specific wiring of stress response and signaling pathways beyond what was expected by sequence orthology, indicating that rewiring of protein interactome networks in related species is likely to be a major factor for divergence. We also identified a previously unknown component Snr1 of the Sty1 mitogen-activated protein kinase (MAPK) pathway and experimentally validated that Snr1 has gained functions, through rewiring of its interactions, compared to the orthologous protein in *S. cerevisiae*. Furthermore, to better understand the evolution of proteins and their interactions, we developed a large-scale cross-species interactome mapping approach to directly test interactions between *S. pombe* proteins and the *S. cerevisiae* orthologs of their partners. Such analysis is only possible with the availability of two well-controlled high-coverage interactome maps generated with the same technology. We found that, for many conserved interactions, both partners had coevolved to accommodate new interactions and functions, and their interaction interfaces can no longer be recognized by their *S. cerevisiae* counterparts.

RESULTS

Comparison of known interactions in *S. cerevisiae* and *S. pombe*

The number of known protein-protein interactions in *S. pombe* is disproportionately lower than in other model eukaryotic organisms and human. We estimated the number of all known interactions in *S. cerevisiae* and *S. pombe* by analyzing seven commonly used databases—BioGRID (*16*), DIP (*17*), IntAct (*18*), iRefWeb (*19*), MINT (*20*), MIPS (*21*), and VisANT (*22*). We identified 110,443 interactions for budding yeast, but only 4038 for fission yeast, from these databases. Furthermore, only those interactions or interaction sets that have been validated by at least two independent assays are reliable and defined as "high quality" (*23*, *24*). On the basis of this criterion, 519 fission yeast interactions are of high quality, as opposed to 25,335 high-quality interactions known in budding yeast. Of these, only 160 *S. pombe* interactions are binary (a direct biophysical interaction between the two proteins), as opposed to 11,936 in *S. cerevisiae*. These numbers (table S1) indicate the extent to which the fission yeast interactions are underexplored and necessitate the systematic mapping of its interactome network.

StressNet: A large-scale high-quality protein interactome network for stress response and cellular signaling in *S. pombe*

The subset of 658 genes for this study was selected using Gene Ontology (GO) (*25*) "Biological Process" (BP) functional annotations for fission yeast (Fig. 1A and table S2). To generate a high-quality, high-coverage stress response interactome map for *S. pombe*, we screened all possible protein pairs (>430,000) in this space three times using a high-quality HT-Y2H system, as we had done for *S. cerevisiae* (*1*). The resulting protein interactome network, StressNet (Fig. 1B), comprises 235 high-quality binary interactions among 200 proteins (table S3). Of these, 218 interactions were previously unknown. To validate our experimental pipeline and the quality of StressNet from the 160 high-quality binary interactions, we selected a set of 54 well-documented protein interactions from the literature ["positive reference set" (PRS); table S4] and 43 random protein pairs that have never been reported or predicted to interact ["random reference set" (RRS); table S5]. Twenty PRS interactions were successfully confirmed in our pipeline, whereas none of the RRS pairs were detected as positives (Fig. 1C). Therefore, the sensitivity [fraction of detected true positives among all possible true positives (*1*)] of our Y2H assay is 37.0%.

To directly measure the quality of our Y2H-identified interactions (*1*, *26*), we retested all 235 interactions detected in our HT-Y2H screen by two orthogonal assays: the protein complementation assay (PCA) (*27*) and the well-based nucleic acid programmable protein array (wNAPPA) (*28*), producing a fully verified large-scale interactome map. The confirmation rates of our interactions with both orthogonal assays were similar to those of the PRS, further validating the high quality of StressNet (*1*, *26*) (Fig. 1C). Using the results of the validating assays, we calculated the precision of StressNet as 95.3 ± 4.7% (Eqs. 8 and 9).

To assign a confidence score to each interaction in StressNet, we implemented a random forest algorithm to integrate results from the three orthogonal assays (figs. S1 and S2 and Materials and Methods). Every detected interaction had a confidence score of >0.76 (table S3). This value represents a normalized probability on a scale of 0 to 1 and indicated that

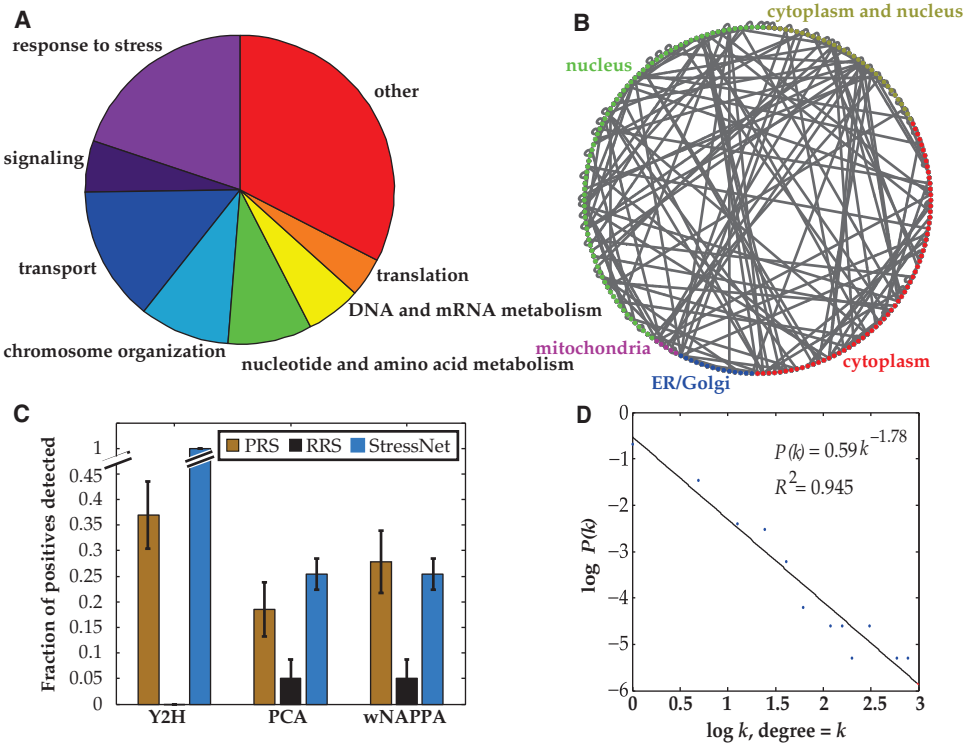

Fig. 1. *S. pombe* stress response binary interactome network, StressNet. (**A**) Functional classification of the proteins included in our high-quality, high-coverage HT-Y2H screen. (**B**) Network view of the stress response binary interactome network in *S. pombe*. (**C**) Fractions of protein pairs in PRS, RRS, and StressNet that tested positive using Y2H, PCA, and wNAPPA. Data are shown as measurements + statistical error (SE). (**D**) Degree distribution of StressNet. *P*(*k*) is the probability that a protein has a degree = *k*.

all the interactions in StressNet were of high quality. Finally, to evaluate the topological properties of our network, we plotted the degree (number of interactions each protein has) distribution of StressNet (Fig. 1D and table S6). Protein interactomes are small-world scale-free networks (*29*, *30*), and our stress response interactome for *S. pombe* exhibited similar topological properties to other large-scale biological networks.

To assess the biological relevance of this network, we investigated the overall relationships between protein pairs using expression and genetic interaction profile similarities (*14*, *31*), subcellular colocalization (*32*), and GO functional similarities (*25*). We found significant enrichment of interactions in StressNet of protein pairs that colocalized or were functionally similar and that were encoded by coexpressed genes or genes that exhibited similar genetic interaction profiles [calculated using the Pearson correlation coefficient (PCC)], relative to random expectation (Fig. 2, A to D). Furthermore, the enrichment of StressNet in all four categories was similar to that of high-quality literature-curated binary interactions. These results confirmed the high quality of StressNet and indicated that these interactions are likely to be functionally relevant.

Evolutionary relationships in StressNet

For biological networks, evolutionary relationships are commonly measured in terms of conservation and rewiring: If a pair of interacting proteins in one species has corresponding orthologs in another that also interact, then the interaction is considered to be conserved (an interolog); otherwise, the interaction is considered to be rewired (*33*–*35*) (Fig. 3A). To understand key principles governing the evolution of protein-protein interactions, especially for those in stress response and signaling pathways, we compared the interactions in StressNet to their corresponding ortholog pairs in *S. cerevisiae*. We experimentally tested all corresponding *S. cerevisiae* protein pairs of the 235 interactions in StressNet and found that for 35 interactions, the corresponding budding yeast ortholog pairs were detected as interacting by our Y2H experiments. We developed a Bayesian framework to calculate the percentage of conserved interactions based on three parameters—the proportion of observed conserved interactions (35/235 = 14.9%) and the precision (95.3 ± 4.7%) and the sensitivity (37.0 ± 4.4%) of our Y2H assay (see Eqs. 12 and 13). Substituting appropriate values, the percentage of conserved interactions between *S. pombe* and *S. cerevisiae* is calculated as 36.3 ± 2.9% (Fig. 3B).

Using an orthogonal approach, we supplemented *S. cerevisiae* interactions detected in our Y2H experiments with high-quality known *S. cerevisiae* interactions curated from the literature to obtain 55 more StressNet interactions for which the corresponding budding yeast orthologs were reported to interact in the literature (*24*). There are 90 (35 + 55) conserved interactions in total (table S7), and the conservation is 38.3 ± 3.2%, consistent with the conservation calculated using the Bayesian framework (Fig. 3B). Furthermore, this agreement shows that after combining our Y2H experimental results with high-quality literature-curated interactions, the number of known interactions in our search space in *S. cerevisiae* is nearly complete, because if there were still a large number of unidentified interactions, the observed proportion of conserved interactions based on literature-curated interactions would have been much lower. Because it is always difficult to determine a negative interaction (*1*, *36*), to ensure the set of rewired interactions is of high quality, we used a stringent set of criteria to define them (table S7) as those StressNet interactions without corresponding *S. cerevisiae* ortholog pairs and those interactions whose corresponding *S. cerevisiae* ortholog pairs have other high-quality interactions but have never been reported as interacting in the literature or tested positive in our Y2H experiments, and these ortholog pairs are known to have different cellular localizations (*37*).

Proteins encoded by essential genes, those when deleted cause lethality, tend to have more interacting partners (hubs) and also evolve more slowly than nonessential ones (*38*, *39*). We found that essential and nonessential genes (*40*) in our interactome were equally likely to be involved in conserved interactions (Fig. 3C), contrary to previous studies (*39*). Stress response and signal transduction pathways play a crucial role in the process of adaptation to distinct ecological environments. As measured by the ratio of nonsynonymous to synonymous substitution rates (d*N*/d*S*)

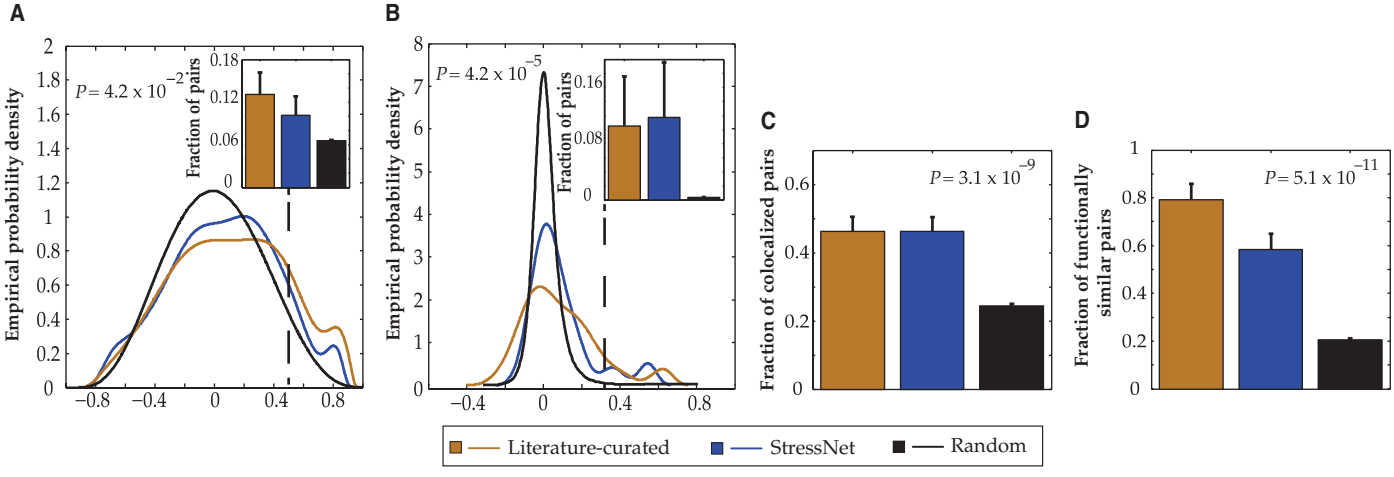

Fig. 2. Biological properties of StressNet interactions. (**A**) PCC distribution of expression profiles of interacting and random protein pairs (dashed line corresponds to PCC cutoff above which pairs are considered to be significantly coexpressed; inset shows the fraction of significantly coexpressed pairs). (**B**) PCC distribution of genetic interaction profiles of interacting and random protein pairs (dashed line corresponds to PCC cutoff above which pairs are considered to be significantly similar; inset shows the fraction of pairs with significantly similar interaction profiles). (**C**) Enrichment of colocalized protein pairs. (**D**) Enrichment of protein pairs sharing similar functions. For each panel, the random set is constructed by considering all pairwise combinations of genes or proteins in the corresponding space. All *P* values represent comparisons between StressNet interactions and random pairs using a cumulative binomial test. Inset graphs and data in (C) and (D) are shown as measurements + SE.

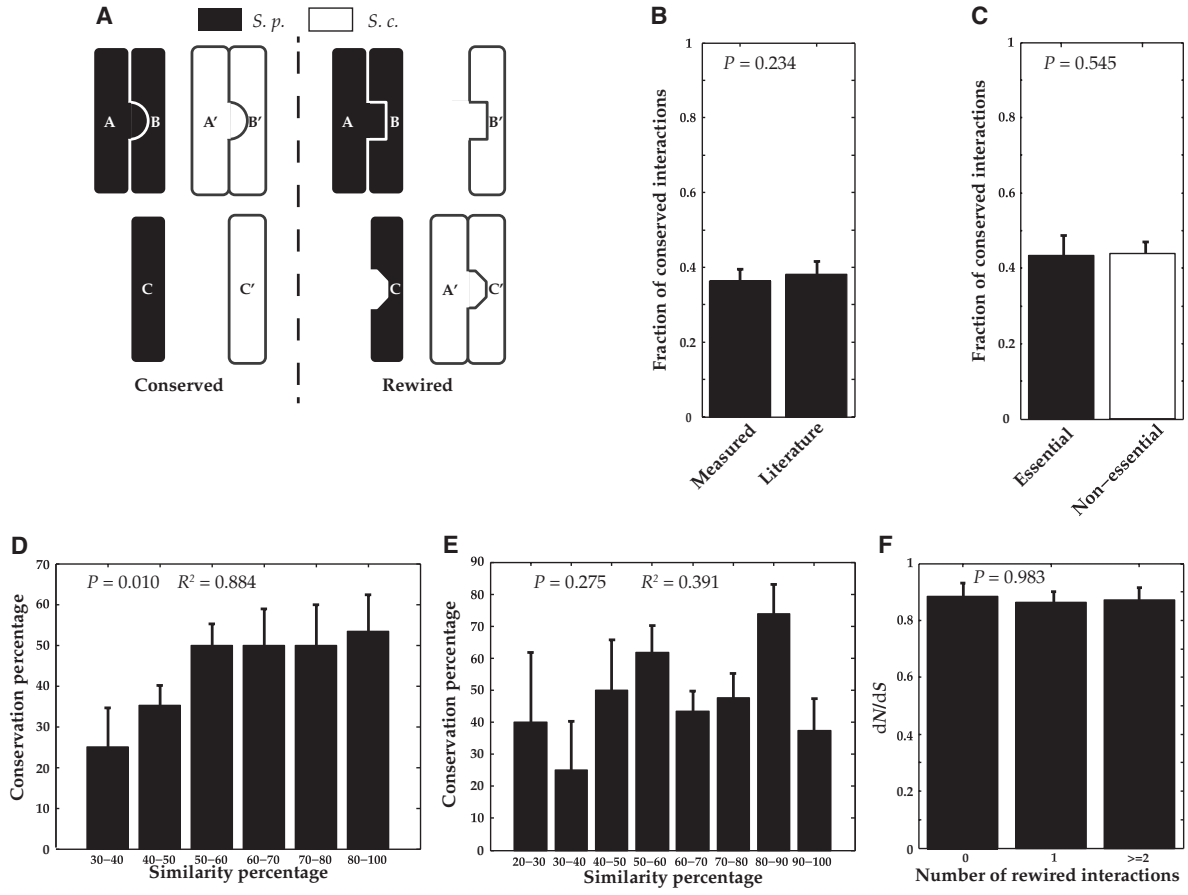

Fig. 3. Evolutionary analysis of interactions. (A) Schematic of conserved and rewired interactions between the two yeast species. *S.p.*, *S. pombe*; *S.c.*, *S. cerevisiae*. (B) Conservation rate (fraction of conserved interactions) in our interactome calculated in two different ways. Measured represents the value calculated using a Bayesian framework that incorporates the precision and recall of our assay. Literature represents the value estimated using budding yeast interactions reported in the literature. (C) Fractions of conserved interactions involving essential and nonessential proteins. The differences in (B) and (C) are not significant based on a cumulative binomial test. (D) Distribution of the fraction of conserved interactions as a function of overall sequence similarity. (E) Distribution of the fraction of conserved interactions as a function of sequence similarity of interaction interfaces. For (D) and (E), *P* values are used to test whether there is a significant difference (using a cumulative binomial test) in conservation percentage between the groups corresponding to the lowest and highest similarity percentages. R^2 (coefficient of determination) represents the significance of the correlation between conservation and similarity percentages. (F) Distribution of d*N*/d*S* [ratio of the number of nonsynonymous substitutions per nonsynonymous site (d*N*) to the number of synonymous substitutions per synonymous site (d*S*)] as a function of the number of rewired interactions. Differences are not significant as determined by a two-sided Kolmogorov-Smirnov test. Data are shown as measurements + SE.

(*41*, *42*), we found that the essential genes in these pathways evolve at the same rate as the nonessential genes in the pathways evolve, although, on average, all essential genes in the genome evolve significantly slower (fig. S3) than do nonessential genes. To ensure that this is not an artifact of the calculation method, we also calculated the d*N*/d*S* values for all essential and nonessential genes. Consistent with earlier findings (*24*), we observed that, overall, the essential genes had a significantly lower average d*N*/d*S* (fig. S3). The average d*N*/d*S* for all stress response genes is not significantly different from that for the entire genome (fig. S4). The d*N*/d*S* distributions for these two species are highly similar (fig. S5). This finding is consistent with analyses that suggest that these species are at comparable evolutionary distances from *S. pombe* (*21*, *22*) and confirm that there are no inherent biases in our d*N*/d*S* calculations. Thus, our findings suggest that essential genes in stress response and signal transduction pathways are under less negative selection such that their interactions are rewired for adaptive advantages through evolution.

To better understand the mechanisms underlying conservation and rewiring of interactions, we examined the relationship between sequence similarity of orthologous pairs and interaction conservation rates. Consistent with expectation (*33*), interactions involving proteins with higher overall sequence similarity or identity were more likely to be conserved (Fig. 3D and fig. S6). However, proteins interact through specific domains (*43*); therefore, we examined the role of sequence similarity of these interfaces in determining the conservation of corresponding interactions. Previous studies have established a homology modeling approach (*44*, *45*) to locate interaction interfaces using cocrystal structures in the Protein Data Bank (*46*) and have found that analysis of these interfaces provides insights into their evolutionary rate (*44*). The conservation of an interaction depends on the conservation of the interfaces involved (*47*). Using a

similar approach, we inferred interaction interfaces for proteins involved in 161 interactions in our network (Materials and Methods). We found no significant correlation between the similarity or identity of interaction interfaces and the conservation of the corresponding interactions (Fig. 3E and fig. S6). Examination of the average d*N*/d*S* ratios for proteins with different numbers of rewired interactions showed that the selection pressure on the gene did not affect the degree to which the interactions of the corresponding protein were rewired (Fig. 3F), further indicating that the rewiring of interactome networks and the divergence of related species are not completely dictated by evolution detected at the sequence level.

Functional profile of conserved and rewired interactions

To investigate whether gene pairs encoding proteins involved in conserved and rewired interactions are differently regulated at the transcriptional level, we measured global coexpression between these pairs using the PCC. Global coexpression means that the patterns of gene expression of both genes are the same (fig. S7). Whereas conserved interactions had the highest fraction of coexpressed pairs, gene pairs encoding proteins involved in rewired interactions were also significantly more coexpressed than random in *S. pombe* (Fig. 4A). We also calculated coexpression relationships for the corresponding budding yeast pairs. By definition, the conserved pairs also interact in budding yeast, but the rewired pairs do not. The enrichment in gene expression is consistent with this distinction: Gene pairs encoding proteins involved in conserved interactions were coexpressed, and genes encoding rewired pairs were not significantly more enriched than random expectation in *S. cerevisiae* (Fig. 4A).

PCC captures only global coexpression relationships but cannot capture local or transient coexpression that occurs only under certain conditions (fig. S7). Furthermore, gene pairs encoding proteins involved in stable interactions tend to be globally coexpressed, whereas those in transient interactions are often only locally coexpressed without significant PCC values (*48*). Stable and transient interactions both have important biological functions—the former constitute tightly connected modules, whereas the latter form key links between modules, especially in signal transduction pathways, and are more important than the stable ones or random interactions in maintaining the integrity of cellular networks (*48*). To detect transient interactions, we used the local expression-correlation scores (LES) (*48*, *49*). Rewired interactions in fission yeast had significantly higher LES values (Fig. 4B) than both conserved interactions and random expectation, suggesting that transient interactions are more likely to be rewired through evolution. Rewired pairs in budding yeast had lower LES values than random pairs (Fig. 4B), indicating that gene regulation for these pairs is also rewired.

Next, we examined the GO functional similarities between interacting proteins involved in conserved and rewired interactions. Whereas conserved interactions had higher functional similarity than rewired interactions in fission and budding yeast, interacting protein pairs in both categories were significantly more functionally similar than random (Fig. 4C). This is in agreement with previous findings that conserved interactions tend to be in modules with specific functions, whereas rewired interactions tend to be intermodular and have greater diversity in function (*48*).

In our analysis of rewired interactions above, we focused on those that are present in fission yeast but lost in budding yeast. Because the *S. pombe* interactome is still considerably underexplored in the literature and the sensitivity of our Y2H assay is 37.0%, it is not yet possible to determine noninteracting pairs in *S. pombe* reliably. Therefore, although it is possible to define lost interactions in *S. cerevisiae* by combining literature-curated interactions with our Y2H-detected ones, the same cannot be done to define lost interactions in *S. pombe*. However, there are 1638 *S. cerevisiae* interactions where one protein has a corresponding *S. pombe* ortholog in the space of the 658 open reading frames (ORFs) that we explored and another protein has no *S. pombe* ortholog. Thus, there can be no corresponding *S. pombe* interactions, and these are rewired interactions in *S. cerevisiae* by definition. We found that these rewired interactions had significantly higher PCC, LES, and functional similarity compared to random (fig. S8). The trend is comparable to that of rewired interactions in *S. pombe* (Fig. 4), further confirming the robustness of our results. We performed PCC and LES analysis of coexpression (fig. S9) and functional similarity (fig. S10) of conserved and rewired interactions defined at different confidence levels and obtained similar results, indicating that the analysis is robust and reliable.

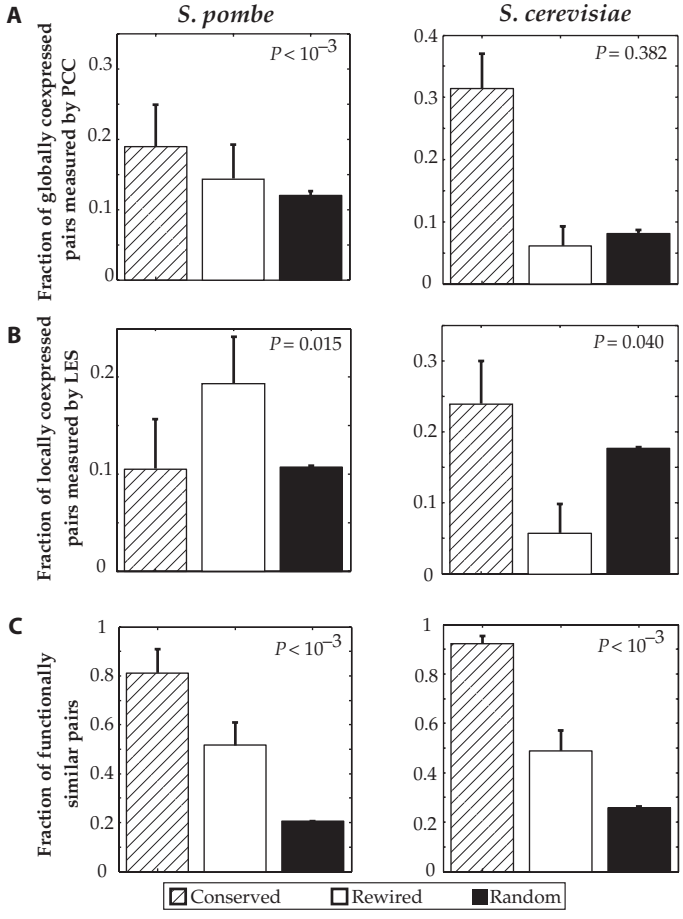

Fig. 4. Functional analysis of conserved and rewired interactions in *S. pombe* and *S. cerevisiae*. (A) Fractions of globally coexpressed pairs (as measured by PCC) among conserved and rewired interactions. (B) Fractions of locally coexpressed pairs (as measured by LES) among conserved and rewired interactions. (C) Fractions of functionally similar pairs among conserved and rewired interactions. For each panel, the random set is constructed by considering all pairwise combinations of genes/proteins in the corresponding space. All *P* values represent comparisons between rewired interactions and random pairs using a cumulative binomial test. Data are shown as measurements + SE.

Modes of rewiring uncovered by cross-species interactome mapping

To further understand the meaning of "conservation" of interactions and experimentally explore the molecular mechanisms through which interaction interfaces evolve, we performed a systematic cross-species interactome mapping by testing all conserved interactions between corresponding *S. cerevisiae* and *S. pombe* proteins. Using orthologous pairs of interacting proteins in the two yeast species, we examined whether a protein in one species interacted with the ortholog of its partner in the other (Fig. 5A). Because we could detect the original interacting pairs from the same species with our Y2H experiments, we know that all four proteins are correctly expressed, folded, and amenable to detection by our Y2H approach, thereby avoiding technical false negatives. The traditional definition of conservation implies the notion of conserved interfaces across different species. However, there are many examples where proteins with conserved interactions form new interactions and carry out new functions that are not conserved. The interface of a conserved interaction in fission yeast is considered "intact" if the proteins involved could also interact with the corresponding orthologs of their partners in budding yeast; otherwise, the interface is considered "coevolved" (Fig. 5A). We found that these conserved interactions equally likely result from an intact interface or coevolved interface that formed new interaction interfaces that were unrecognizable by their orthologous counterparts in the other species (Fig. 5B). Earlier studies have suggested that interacting proteins may coevolve to maintain structural complementarity and binding specificity (*50*–*52*). In this calculation, we used a lenient definition for an intact interface: We considered the interface intact if one or both of the cross-species interactions were positive, which provides a lower bound estimation of coevolution between interacting proteins.

Divergence of the Sty1 stress response pathway through interaction conservation and rewiring

In *S. pombe*, Sty1 is activated in response to various stresses, including oxidative and osmotic stress, starvation, and other conditions (*53*, *54*). Sty1 has orthologs in *S. cerevisiae* (Hog1, with 89% sequence similarity) and human (p38, with 69% sequence similarity). Both p38 and Sty1 respond to a wide range of stresses, and both are different from Hog1 in terms of function (*55*). With our stress response interactome, we detected key interactions at every step of the MAPK signal transduction pathway and, therefore, completely recapitulated the entire Sty1 pathway (fig. S11). This confirmed the sensitivity and accuracy of our HT-Y2H method, especially

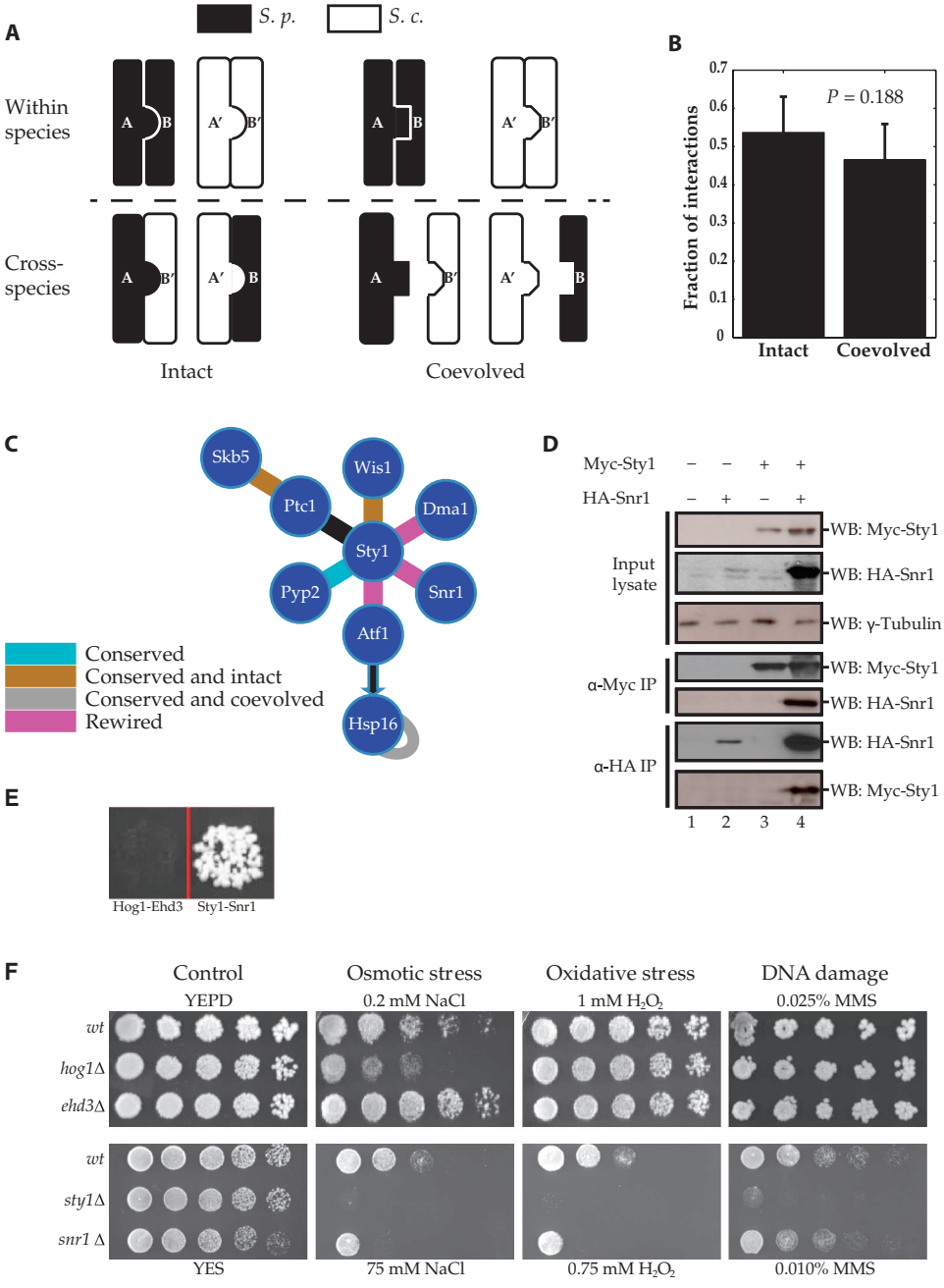

Fig. 5. Analysis of intact and coevolved interactions. (A) Schematic of intact and coevolved interactions. (B) Fractions of intact and coevolved interactions in our interactome. Data are shown as measurements + SE. No significant difference detected by a cumulative binomial test. (C) The MAPK Sty1 stress response pathway. All undirected lines represent interactions detected in our interactome. Black arrow represents transcriptional regulation. (D) Sty1-Snr1 interaction validated in *S. pombe* by coimmunoprecipitation ($n = 3$ blots). (E) Y2H analysis of the ability of Hog1 and Ehd3 to interact and of Sty1 and Snr1 to interact ($n = 3$ experiments). (F) Sensitivity assays for different deletion strains of *S. cerevisiae* and *S. pombe* under various stress conditions ($n = 3$ experiments).

for discovering transient interactions in signaling pathways. Among all Sty1 interactions in StressNet, those with its activator (Wis1) and inhibitor (Pyp2) were both conserved between the two yeast species, and the Sty1-Wis1 interaction interface was intact. By contrast, the interaction between Sty1 and its known target in fission yeast, Atf1, represented a rewired interaction (Fig. 5C). We also identified a previously unknown interactor of Sty1: SPBC2D10.09, a protein that we named Snr1 (Sty1-interacting stress response protein). To confirm this interaction in vivo, we performed coimmunoprecipitation of tagged proteins expressed in *S. pombe* (Fig. 5D and table S8). The amount of Snr1 pulled down in the presence of Sty1 was greater than that pulled down in the absence of Sty1, indicating that the interaction with Sty1 stabilizes Snr1 (Fig. 5D). The corresponding orthologous pair of Hog1 and Ehd3 in *S. cerevisiae* did not interact by Y2H (Fig. 5E). Cells lacking *snr1* (*snr1*Δ cells) grew slower under stress, similar to *sty1*Δ cells (Fig. 5F and fig. S12), whereas the growth of *ehd3*Δ cells was not compromised. These results suggested that Snr1 is a component of the Sty1 pathway and that its functions diverged from its budding yeast counterpart. Moreover, *snr1* also has a human ortholog, HIBCH, further investigation of which may expand our knowledge of the human p38 MAPK pathway.

DISCUSSION

We generated StressNet—a high-quality, high-coverage binary interactome for stress response and signal transduction pathways in the fission yeast *S. pombe*. All interactions were verified by three orthogonal assays and assigned probabilistic confidence scores. We performed comparative network analysis to study the evolution of protein interactomes between the fission and budding yeast species. Although 84% of StressNet interactions have corresponding orthologous pairs in *S. cerevisiae*, only about 40% of these interactions are conserved, indicating considerable evolutionary changes beyond simple sequence orthology. Thus, the interolog concept should be used with caution to infer interactions across species, especially if the two are not closely related. Furthermore, our results suggest that rewiring of protein interactome networks in related species is likely a major factor for divergence. Surprisingly, we found no significant correlation between the similarity of interaction interfaces and the conservation of corresponding interactions. This demonstrates that conservation of interactions is more complex than previously expected—domains that are not part of the interaction interface also play some indirect role in making the interaction possible. Even if the interface is conserved, the corresponding interaction could still be rewired because of steric hindrance due to altered overall structure or loss of nearby structural scaffolds that make the interaction thermodynamically favorable (*56*). We also experimentally explored the evolution of interaction interfaces, and our analysis indicated that interactions traditionally considered "conserved" are equally likely to have intact interfaces as to have coevolved ones that are different from their orthologous counterparts. These results suggest a molecular mechanism by which the interactome network is rewired through evolution: Many proteins have coevolved with their partners to form modified interfaces that can, therefore, accommodate new interactions and functions.

Our results indicated that conserved interactions tended to be stable, and rewired ones were more likely to be transient. Therefore, our finding provides a molecular-level mechanistic explanation for previous studies showing that genetic cross talk between functional modules can differ substantially (*14*, *57*, *58*). However, our results also suggest that, overall, proteins tend not to rewire all of their interactions; thus, even if they acquire novel interactions, they still generally conserve at least some of the original functions.

Our results indicate that substantial evolutionary changes, both rewiring and coevolution, of stress response pathways could be a major mechanism by which different organisms adapt to diverse living environments. Conservation of interactions in other pathways might be different from what we observed here. Therefore, similar cross-species interactome mapping and comparative network analyses of more pathways and species will provide a more comprehensive understanding of underlying principles that help shape distinct characteristics of individual organisms through evolution.

MATERIALS AND METHODS

Selection of genes for the study

This study focused on stress response and signal transduction proteins (based on GO Biological Process annotations) and their known interactors in *S. pombe*. We also included *S. pombe* orthologs of *S. cerevisiae* proteins that are known to interact with orthologs of fission yeast stress response and signal transduction proteins. While selecting the 658 ORFs (table S2), we also ensured that a set of PRS interactions in *S. pombe* could be constructed with genes from our space, a limiting criterion because there are only 160 binary high-quality *S. pombe* interactions reported in the literature.

Yeast two-hybrid

Y2H experiments were carried out as described (*59*). Briefly, 658 *S. pombe* ORFs in Gateway entry vectors were transferred into AD and DB vectors using Gateway LR reactions. After bacterial transformation, plasmids of all AD-Y and DB-X clones were transformed into Y2H strains *MAT***a** Y8800 and *MAT*α Y8930 (genotype: *leu2-3, 112 trp1-901 his3*Δ*200 ura3-52 gal4*Δ *gal80*Δ *GAL2-ADE2 LYS2::GAL1-HIS3 met2::GAL7-lacZ cyh2*^{R}), respectively. The *MAT***a** Y8800 strain was obtained from the *MAT***a** Y550 strain after mutating *CYH2* to introduce cycloheximide (CHX) resistance. *MAT*α Y8930 was generated by crossing *MAT***a** Y8800 with *MAT*α Y1541 (*3*), followed by sporulation and identification of the *MAT*α CHX-resistant yeast strain by tetrad analysis. After AD-Y and DB-X were transformed into Y8800 and Y8930, respectively, autoactivators were screened by spotting onto synthetic complete medium (SC) lacking histidine and tryptophan (AD-Y) or histidine and leucine (DB-X). These autoactivators were excluded from all further screenings. Each unique DB-X was mated with pools of ~188 unique AD-Y by co-spotting onto yeast extract peptone dextrose (YEPD) plates. Diploids were selected by replica plating onto SC plates without leucine and tryptophan (SC−Leu−Trp). To select for positive interactions, we performed Y2H screening by replica plating the diploids onto SC plates with 1 mM 3-amino-1,2,4-triazole (3-AT) and without leucine, tryptophan, and histidine (SC−Leu−Trp−His+3-AT). SC−Leu−Trp−His plates were used for the HT-Y2H screen in *S. cerevisiae* (*1*). We used 1 mM 3-AT because this concentration greatly reduces background and improves the quality of the screens (*8*, *59*, *60*). Newly occurring autoactivators were determined by concurrently replica plating the diploids onto SC medium with CHX and 1 mM 3-AT and lacking leucine and histidine (SC−Leu−His+3-AT+CHX). Screening for these autoactivators relies on CHX to select for cells that do not have the AD plasmid because of plasmid shuffling. Thus, growth on the latter plate identifies spontaneous autoactivators; these were removed from further analyses. All plates were replica cleaned the following day and scored after three additional days. The space was screened three times.

Y2H positives were grown 2 to 3 days at 30°C and then spotted onto four plates for secondary phenotype confirmation (phenotyping II) (SC−Leu−Trp−His+3-AT; SC−Leu−His+3-AT+CHX; SC−Leu−Trp−adenine; SC−Leu−adenine+CHX). Colonies that either grew on SC−Leu−Trp−His+3-AT but not on SC−Leu−His+3-AT+CHX or grew on SC−Leu−Trp−adenine but not on SC−Leu−adenine+CHX were identified as positives.

For colonies that scored positive in phenotyping II, the identities of DB-X and AD-Y were determined by the Stitch-seq approach (*59*) using Illumina sequencing. All identified interacting pairs were retested by pairwise Y2H.

Construction of PRS and RRS

The PRS and RRS are representatives of true-positive interactions and negative pairs, respectively, and we used the PRS and the RRS to optimize the assay performance, and they may be interpreted as positive and negative controls. The PRS comprises a set of 54 protein interactions from the literature, each of which is supported by at least two independent assays from two different publications (table S4). RRS pairs were generated from a random selection out of all possible protein pairs within our search space for which no interaction has yet been detected by any method (table S5). Because fission yeast interactions are underexplored, we also required that their corresponding budding yeast ortholog pairs have never been reported to interact.

Another way to construct the RRS is to consider protein pairs with different cellular localizations because these are unlikely to interact. Thirty-one of the 43 RRS pairs are indeed localized in different cell compartments. Using the whole RRS (Fig. 1C), we estimated the false-positive rates for Y2H, PCA, and wNAPPA to be 0/43, 2/43 (4.7 ± 3.2%), and 2/43 (4.7 ± 3.2%), respectively. If we only use the 31 RRS pairs localized in different cell compartments (named "RRS_DiffLocal"), the false-positive rates for the three assays are 0/31, 2/31 (6.5 ± 4.4%), and 1/31 (3.2 ± 3.2%). Therefore, the false-positive rates for all three assays used in our experiments do not change whether we use the complete RRS or RRS_DiffLocal.

With these controls, we found that 20 of the 54 PRS, and none of the RRS, were detected in our screen. We calculated the sensitivity of our assay as 20/54 (37.0 ± 4.4%).

Protein complementation assay

S. pombe ORFs available in Gateway entry vectors were transferred by Gateway LR reactions into vectors encoding the two fragments of YFP (Venus variant) fused to the N terminus of the tested proteins. Baits were fused to the F1 fragment (amino acids 1 to 158 of YFP), and preys were fused to the F2 fragment (amino acids 159 to 239 of YFP). After bacterial transformation, plasmid DNA was prepared on a Tecan Freedom Evo biorobot, and DNA concentrations were determined by the absorbance at 260 nm (A_{260}) with a Tecan M1000 in a 96-well format. A 50-ng aliquot of each vector encoding the two proteins was used for transfection into human embryonic kidney 293T cells in 96-well plates, using Lipofectamine 2000 (Invitrogen) reagent according to the instructions of the manufacturer. At about 48 hours after transfection, cells were processed with a Tecan M1000. A pair is considered interacting if the YFP fluorescence intensity was ≥2-fold higher over background.

Well-based nucleic acid programmable protein array

ORFs encoding the interacting proteins were cloned into Gateway-compatible pCITE-HA (hemagglutinin) and pCITE-GST (glutathione *S*-transferase) vectors by LR reactions. After bacterial transformation, growth, DNA minipreps, and determination of DNA concentration, ~0.5 μg of each plasmid was added to Promega TnT coupled transcription-translation mix (catalog no. L4610) and incubated for 90 min at 30°C to express proteins. During this time, anti-GST antibody–coated 96-well plates (Amersham 96-well GST detection module, catalog no. 27-4592-01) were blocked at room temperature with phosphate-buffered saline containing 5% dry milk powder. After protein expression, the expression mix was diluted in 100 μl of blocking solution and added to the emptied preblocked 96-well plates. Expression mix was incubated in the 96-well plates for 2 hours at 15°C with agitation to allow for protein capture. After capture, plates were washed three times and developed by incubation with primary and secondary antibodies. Signal was visualized by chemiluminescence (Amersham ECL reagents, catalog no. RPN2106) with a Tecan M1000 plate reader. Wells with ≥3-fold higher intensity over background in either configuration were considered positives.

Measuring the precision of our assay

The precision of the Y2H assay was calculated using PCA and wNAPPA as orthogonal validation assays. Using Bayes' rule, we can build relationships between the true- and false-positive rates of Y2H and observed positive interactions by a validating assay as follows:

$$\Pr(A+|Y+) = \Pr(A+|Y+,T+) \times \Pr(T+|Y+) + \Pr(A+|Y+,T-) \times \Pr(T-|Y+) \quad (1)$$

where A+ corresponds to observing a positive interaction using the validating assay, Y+ corresponds to observing a positive interaction using Y2H, and T+ (T−) corresponds to an interaction being a real positive (negative) interaction. The precision of the Y2H is the term Pr(T+|Y+) [which is also equal to 1 − Pr(T−|Y+)].

Assuming conditional independence between the validating assay and Y2H on the basis of previously defined reasons (*1*), we can write

$$\Pr(A+|Y+) = \Pr(A+|T+) \times \Pr(T+|Y+) + \Pr(A+|T-) \times \Pr(T-|Y+) \quad (2)$$

Solving for the precision of the Y2H assay yields

$$\Pr(T+|Y+) = \frac{\Pr(A+|Y+) - \Pr(A+|T-)}{\Pr(A+|T+) - \Pr(A+|T-)} \quad (3)$$

Pr(A+|T+) and Pr(A+|T−) were measured in the PRS and RRS experiments. So, for our Y2H assay, we can write precision as

$$\text{Precision} = \frac{F_{\text{StressNet}} - F_{\text{RRS}}}{F_{\text{PRS}} - F_{\text{RRS}}} \quad (4)$$

where $F_{\text{StressNet}}$ is the fraction positive by an assay for StressNet, which is the best estimator for Pr(A+|Y+). F_{PRS} is the fraction positive by the assay for the PRS, which is an estimator for Pr(A+|T+). F_{RRS} is the fraction positive by the assay for the RRS, which is an estimator for Pr(A+|T−).

The standard errors of $F_{\text{StressNet}}$, F_{PRS}, and F_{RRS} are calculated using the standard error for binomial distributions:

$$\text{StdErr} = \sqrt{\frac{F(1-F)}{N}} \quad (5)$$

where F is the fraction positive by the assay ($F_{\text{StressNet}}$, F_{PRS}, or F_{RRS}) and N is the total number of pairs tested.

To estimate the standard error for the precision, we used the standard delta method:

$$\sigma_X^2 = \left(\frac{\partial f}{\partial A}\sigma_A\right)^2 + \left(\frac{\partial f}{\partial B}\sigma_B\right)^2 + \left(\frac{\partial f}{\partial C}\sigma_C\right)^2 + \ldots \quad (6)$$

where $X = f(A, B, C, \ldots)$. $A, B, C, \ldots$ are independent random variables.

Here, the standard error of the precision is calculated as:

$$\sigma_{\text{precision}} = \sqrt{\left(\frac{1}{F_{\text{PRS}} - F_{\text{RRS}}}\right)^2 \times \sigma^2_{\text{StressNet}} + \frac{(F_{\text{StressNet}} - F_{\text{RRS}})^2}{(F_{\text{PRS}} - F_{\text{RRS}})^4} \times \sigma^2_{\text{PRS}} + \frac{(F_{\text{StressNet}} - F_{\text{PRS}})^2}{(F_{\text{PRS}} - F_{\text{RRS}})^4} \times \sigma^2_{\text{RRS}}} \quad (7)$$

We have two validating assays, and we can incorporate the precision rates from these assays by calculating the average precision:

$$\text{Average Precision} = \frac{\text{Precision}_{\text{PCA}} + \text{Precision}_{\text{wNAPPA}}}{2} \quad (8)$$

The standard error for the average precision is calculated by the delta method as

$$\sigma_{\text{average precision}} = \sqrt{\frac{\sigma^2_{\text{PCA}}}{4} + \frac{\sigma^2_{\text{wNAPPA}}}{4}} \quad (9)$$

Using this framework, we estimate the precision of our Y2H assay to be 95.3 ± 4.7%.

Calculating confidence scores for interactions

Using the random forest algorithm (*61*), we integrated the results from Y2H, PCA, and wNAPPA and calculated the confidence scores for interactions. Random forest is an ensemble classifier that constructs multiple decision trees by stochastic discrimination (*62*) and predicts a final class on the basis of a weighted combination of the output class of each decision tree. It is considered to be a robust and accurate classifier for noisy data sets (*61*). We evaluated the performance of our classifier by fivefold cross-validation on our reference set (union of PRS and RRS) and obtained moderately good performance (AUC = 0.64; fig. S2).

Determination of orthologs between *S. pombe* and *S. cerevisiae*

We used the list of orthologs provided by PomBase (*63*). The genome of *S. cerevisiae* underwent a duplication event (*64*). Thus, many *S. pombe* genes have two corresponding *S. cerevisiae* orthologous genes. Moreover, in a number of cases, the same *S. cerevisiae* gene has multiple *S. pombe* orthologs. Thus, the mapping considered for the study was "many-to-many."

Estimation of the conservation of interactions

To estimate the conservation of protein-protein interactions between *S. pombe* and *S. cerevisiae*, we used a Bayesian framework that incorporates the precision and sensitivity of our Y2H assay:

$$\Pr(\text{Det}) = \Pr(\text{Det}|\text{Cons}+) \times \Pr(\text{Cons}+) + \Pr(\text{Det}|\text{Cons}-) \times \Pr(\text{Cons}-) \quad (10)$$

where Pr(Cons+) corresponds to the conservation of protein-protein interactions between *S. cerevisiae* and *S. pombe*. The best estimator for Pr(Det) (the probability of detecting a *S. cerevisiae* interaction among proteins pairs that are orthologous to an interacting protein pair in StressNet) is F_{det}, the fraction of the 235 StressNet interactions in *S. pombe* with corresponding Y2H-detected interactions in *S. cerevisiae* (35/235). Pr(Det|Cons+) and Pr(Det|Cons−) are estimated by F_{PRS} and F_{RRS}, the fractions of PRS and RRS interactions detected by our Y2H assay (20/54 and 0/43, respectively). By definition,

$$\Pr(\text{Cons}+) = 1 - \Pr(\text{Cons}-) \quad (11)$$

We can simplify the earlier equation to obtain an expression for Pr(Cons+):

$$\Pr(\text{Cons}+) = \frac{\Pr(\text{Det}) - \Pr(\text{Det}|\text{Cons}-)}{\Pr(\text{Det}|\text{Cons}+) - \Pr(\text{Det}|\text{Cons}-)} \quad (12)$$

To estimate the error for the conservation percentage, we used the standard delta method as described earlier. The standard deviation of Cons+ is given by

$$\sigma_{\text{Cons}+} = \sqrt{\frac{(F_{\text{PRS}} - F_{\text{RRS}})^2\sigma^2_{F_{\text{det}}} + (F_{\text{det}} - F_{\text{RRS}})^2\sigma^2_{F_{\text{PRS}}} + (F_{\text{det}} - F_{\text{PRS}})^2\sigma^2_{F_{\text{RRS}}})}{(F_{\text{PRS}} - F_{\text{RRS}})^4}} \quad (13)$$

Using the Y2H data, we calculated a conservation of 36.3 ± 2.9% interactions.

Another approach for measuring the conservation is to calculate fraction of *S. cerevisiae* interactions conserved in *S. pombe*. We mapped all *S. pombe* proteins in our space to their corresponding *S. cerevisiae* orthologs. We calculated the number of interactions in this *S. cerevisiae* space detected by our Y2H assay. We then mapped all the observed *S. cerevisiae* interactions to their corresponding *S. pombe* ortholog pairs and calculated the number of pairs detected as interacting in StressNet. We found that for 48/386 (12.4%) *S. cerevisiae* interactions, the corresponding *S. pombe* ortholog pairs also interact. Using the Bayesian framework described above, we calculated the conservation between *S. pombe* and *S. cerevisiae* interactions as 34.7 ± 2.0%, which was statistically the same ($P = 0.708$ using a cumulative binomial test) as the conservation calculated using the Y2H results (36.3 ± 2.9%).

Interaction conservation and confidence scores

After supplementing our Y2H experiments with high-quality interactions from the literature, we find that 90/235 (38.3%) interactions are conserved in StressNet. The statistical error associated with this measurement is related to the sample size and is calculated as the standard error [standard error = standard deviation/square root (N), where N is the number of samples]. The standard deviation is calculated on the basis of the underlying probability distribution. The conservation percentage is obtained by a simple division (90/235 = 38.3%), and the underlying probability distribution is binomial (because each interaction can either be conserved or not, it corresponds to a Bernoulli event, the ensemble of which is modeled by a binomial distribution). The standard error is calculated using the appropriate formula for a binomial distribution: square root $[p \times (1 - p)/N] = 3.2\%$, where p is the fraction of interactions that are conserved (90/235) and N is sample size (235).

To test whether interactions with higher confidence scores were more likely to be conserved, we divided all StressNet interactions into two groups. The first group comprises interactions with confidence scores in the lower two quartiles, and the second group comprises interactions with confidence scores in the upper two quartiles. We then compared the conservation for these two groups. We find that there is no significant difference ($P = 0.37$ using a two-sided Fisher's exact test) in conservation rate between the two groups. This validates that the observed conservation rate is robust and not correlated with the confidence score associated with each interaction.

Evolutionary rates of genes and protein interactions

The evolutionary rate of genes is commonly measured in terms of the ratio of asynchronous nucleotide substitutions per asynchronous site to synchronous substitutions per synchronous site, or d*N*/d*S*. This quantifies the selective evolutionary pressure on certain protein-coding genes to diverge faster, as opposed to others that may almost remain unchanged across species (*20*). To calculate the d*N*/d*S* values for all *S. pombe* genes, we used two sequenced species in the *Schizosaccharomyces* genus—*S. cryophilus* and *S. octosporus* (*21*, *22*). To determine orthology relationships, we used BLAST-x with default parameters (*23*) on all *S. pombe* genes. The top BLAST hit for each *S. pombe* gene against the indexed database of

proteins for each of the two species was designated to be an ortholog, provided the *E* value of the hit was <0.05. Although the *E*-value cutoff is relatively high, it ensures that no potential pairs are missed. For pairs that have been incorrectly estimated to be orthologs, there is a correction step in downstream calculations that will return a d*N*/d*S* value of NaN (not a number) because of too high divergence. For all orthologous pairs, the Nei-Gojobori algorithm (*20*), which uses the Jukes-Cantor substitution model, was used to calculate d*N*/d*S* values.

Conservation of interactions and sequence similarity

Sequence similarity between *S. pombe* ORFs and their *S. cerevisiae* orthologs was measured by performing pairwise sequence alignment between all known ortholog pairs using the Needle program in the EMBOSS suite (*65*). It uses the Needleman-Wunsch alignment algorithm (*66*) to find the optimum alignment of two sequences along their entire length. The recommended default parameters—an affine gap penalty model (*67*) with an opening penalty of 10 and an extension penalty of 0.5 and the BLOSUM62 scoring matrix (*68*)—were used for the alignment. Because the lengths of orthologs may be dissimilar, we calculated the overall similarity percentage (OPS) with reference to the length of the *S. pombe* ORFs:

$$\mathrm{OPS} = \frac{N_{st}}{L\_\mathrm{Sp_t}} \quad (14)$$

where N_{st} is the total number of similar residues and $L\_\mathrm{Sp_t}$ is the total length of the *S. pombe* ORF.

We then examined the relationship between the similarity percentage and the percentage of conserved interactions. Because the number of interactions varies considerably across different groups corresponding to different similarity percentages, we required each group to have at least five interactions. If any group had less than five interactions, it was merged with the next (higher) group. This ensured that our results were robust to outlier effects. We found that there was an increase in the degree of conservation with an increase in overall sequence similarity. To examine whether the primary cause of this trend is the similarity of conserved domains, we identified domains on ortholog pairs that interact (*69*, *70*). We defined the percentage similarity of interacting domains (PSID) as

$$\mathrm{PSID} = \frac{N_{si}}{L\_\mathrm{Sp_i}} \quad (15)$$

where N_{si} is the number of similar residues in interacting domains and $L\_\mathrm{Sp_i}$ is the sum of the lengths of the interacting domains in *S. pombe*.

We also repeated our analysis using sequence identity instead of similarity (fig. S6).

Inferring interaction interfaces from 3did and iPfam

Here, we used interacting domains identified by 3did (*69*) and iPfam (*70*) to define interaction interface. To verify the reliability of inferring these domain-domain interactions, we performed threefold cross-validation for 1456 interaction pairs that have cocrystal structures. Because there are few cocrystal structures for *S. pombe*, this approach allowed us to obtain a meaningful estimate of the quality of the domain-domain predictions in these two databases. We split the pairs into three subsets such that two subsets were used for training and the third one was the test set. For each interaction pair in the test data set, we scored a successful structural prediction when the predicted domain-domain interaction(s) had at least one cocrystal structure in support of it. We repeated the procedure thrice with each of the three subsets as the test set. Among the 1456 PPI pairs, more than 90% were correctly predicted with corresponding interacting domains, indicating that the predicted interaction interfaces used for our calculations were accurate (*45*).

Robustness of differences between sets of conserved and rewired interactions

To assess the robustness of the differences between sets of conserved and rewired interactions, we constructed different sets of conserved and rewired interactions corresponding to different confidence levels.

We constructed two sets of conserved interactions at different confidence levels—Conserved_HQ and Conserved_All. Conserved_HQ comprises only those interactions with corresponding *S. cerevisiae* ortholog pairs that tested positive in our Y2H experiments or were confirmed by two or more independent orthogonal assays in the literature. Conserved_All comprises all interactions in Conserved_HQ and those *S. cerevisiae* ortholog pairs that have been reported as interacting in the literature by only one assay.

We constructed five sets of rewired interactions at different confidence levels—Rewired_ByDefn, Rewired_HQ, Rewired_LC, Rewired_All_DiffLocal, and Rewired_All. Rewired_ByDefn comprises only those StressNet interactions for which at least one of the interacting proteins does not have a *S. cerevisiae* ortholog, and therefore, no corresponding interaction can exist in *S. cerevisiae*. Thus, these interactions are rewired by definition. Rewired_HQ comprises all interactions in Rewired_ByDefn and those interactions for which the corresponding *S. cerevisiae* ortholog pairs have other high-quality interactions but have never been reported as interacting in the literature or tested positive in our Y2H experiments, and these ortholog pairs are known to have different cellular localizations. Thus, these correspond to *S. pombe* interactions with corresponding budding yeast ortholog pairs that are, in principle, noninteracting because they have different cellular localizations (*1*, *71*), and they participate in well-validated interactions with other proteins but have never been reported to interact in the literature. Rewired_LC comprises all interactions in Rewired_ByDefn and those interactions with corresponding ortholog pairs that have other high-quality interactions but have never been reported as interacting in the literature or tested positive in our Y2H experiments. Rewired_All_DiffLocal corresponds to all interactions in Rewired_ByDefn and those interactions with corresponding ortholog pairs that have different cellular localizations. Rewired_All comprises all interactions that are not in Conserved_All.

Construction of myc-sty1 and HA-snr1 expression clones

S. pombe sty1 and *snr1* genes were polymerase chain reaction (PCR)–amplified using the following primers: sty1-pNCH1472-Forward, sty1-pNCH1472-Reverse, snr1-pSGP73-Forward, and snr1-pSGP73-Reverse (table S8). The *sty1* PCR product was cloned into a pNCH1472-myc vector using the Not I and Sal I restriction sites. The *snr1* PCR product was cloned into a pSGP73-HA vector using the Not I and Bgl II restriction sites. pNCH1472-myc-sty1 and pSGP73-HA-snr1 were single- or double-transformed into *S. pombe* KGY553 [American Type Culture Collection (ATCC)]. Transformed yeast was selected on Edinburgh minimal medium (EMM)−Ura plates for pNCH1472-myc-sty1, EMM−Leu plates for pSGP73-HA-snr1, and EMM−Ura−Leu plates for double transformation.

Coimmunoprecipitation and Western blotting

Transformed yeast (KGY553) containing pNCH1472-myc-sty1 or pSGP73-HA-snr1 or both were cultured overnight in 10 ml of EMM selection medium. Yeast pellets were washed in 5 ml of cold TE buffer before protein extraction. To lyse the cells, we added 1 ml of lysis buffer [50 mM tris-HCl (pH 7.5), 0.2% Tergitol, 150 mM NaCl, 5 mM EDTA, Complete Protease Inhibitor tablet] and 600 μl of glass beads to each tube and mixed

them in a beater for two rounds of 10 min each. Protein extracts were centrifuged for 10 min at 13,200 rpm at 4°C in an Eppendorf 5415R centrifuge. Then, 500 µl of supernatant was immunoprecipitated overnight using 20 µl of EZview Red Anti-c-Myc Affinity Gel (Sigma-Aldrich, E6654) or EZview Red Anti-HA Affinity Gel (Sigma-Aldrich, E6779). The next morning, beads were washed three times with cold lysis buffer before being subjected to SDS–polyacrylamide gel electrophoresis and Western blotting analysis. Primary antibodies used in our analysis were anti–c-Myc (Santa Cruz Biotechnology, sc-789), anti-HA (Roche, 12CA5), and anti–γ-tubulin (Sigma-Aldrich, T5192).

Construction of yeast deletion strains

The *snr1*Δ strain was obtained from the Bioneer *Schizosaccharomyces pombe* Genome-wide Deletion Library. The deletion strain was verified by PCR with primers SpEhd3_Up_Fwd and Sp_Dn_Rev spanning the 3′ end of *snr1* and the region immediately downstream. Primers specific for KanMX4 (KanMX4-Fwd and KanMX4-Rev) were used to detect the deletion cassette. A PCR-based strategy was used to construct the *sty1*Δ strain. Briefly, in the first round of PCR, primers (PFA6a_Sty1_Fwd and PFA6a_Sty1_Rev) with 20–base pair (bp) homology to the regions upstream and downstream of *sty1*, respectively, were synthesized for PCR of the pFA6a-KanMX6 cassette. Primers with 20-bp homology to the pFA6a-KanMX6 were synthesized to PCR 290 bp upstream (Sty1-Del-Up_Fwd and Sty1Del-Up_Rev) and 290 bp downstream (Sty1Del-Dn_Fwd and Sty1Del-Dn_Rev) of *sty1*, not including the *sty1* gene. The three PCR products were stitched together sequentially with a second round of PCR. Stitch PCR of the upstream region and pFA6a-KanMX6 and that of the downstream region and pFA6a-KanMX6 were carried out separately. In the third round of PCR, both upstream and downstream stitched PCR products were further stitched together to produce a final product of pFA6a-KanMX6 flanked on the 5′ and 3′ ends by 290 bp that are homologous to the upstream and downstream regions of chromosomal sty1 (Sty1Del-Up_Fwd and Sty1Del-Dn_Rev). The final PCR product was transformed into *S. pombe* 972 h- canonical wild-type (ATCC). Transformed yeast was selected on yeast extract sucrose (YES) medium plates containing G418 (150 mg/liter). Insertion of the pFA6a-KanMX6 cassette by homologous recombination at the *sty1* locus was verified by PCR with primers to target the entire cassette (Sty1Del-Up_Fwd and Sty1-Del-Dn_Rev) and to target an sty1 internal region of 401 bp (Sty1_Fwd and Sty1_Rev). In addition, *sty1* and *snr1* deletion were performed in *S. pombe* KGY553 (ATCC) wild-type (*h- his3-D1 leu1-32 ura4-D18 ade6-M216*) background using a similar PCR strategy. The sequences of primers used for deletion and verification of strains in this study are listed in table S8.

Stress sensitivity assays

S. cerevisiae was grown in YEPD, and *S. pombe* was grown in YES medium. All yeast strains were initially grown as a starter culture overnight at 30°C. From the starter culture, yeast cells were diluted in fresh medium to an initial A_{600} of 0.2. The cultures were grown to mid-log phase (A_{600} = 0.7). The *S. cerevisiae* and *S. pombe* strains were serially diluted fourfold in sterile water and spotted onto YEPD and YES plates, respectively, containing various stressors. Spotted plates were incubated at 30°C, and yeast growth was assessed after 3 days.

SUPPLEMENTARY MATERIALS

www.sciencesignaling.org/cgi/content/full/6/276/ra38/DC1

Fig. S1. Detection of PRS interactions and RRS pairs by three orthogonal assays.
Fig. S2. Confirmation of the reliability of weights of the interactions.
Fig. S3. Evolutionary rate of essential and nonessential genes using *S. cryophilus* or *S. octosporus* for comparison.
Fig. S4. Evolutionary rate of stress response genes and all genes comparing *S. cryophilus* or *S. octosporus* to *S. pombe*.
Fig. S5. Measurement of evolutionary divergence of *S. pombe* from *S. cryophilus* and *S. octosporus*.
Fig. S6. Conservation as a function of sequence identity of the entire protein or sequence identity of the interacting domains.
Fig. S7. Graphical representation of global and local coexpression of genes that express interacting proteins.
Fig. S8. Functional analysis of conserved and rewired (by definition) interactions in *S. cerevisiae*.
Fig. S9. Fractions of globally and locally coexpressed pairs for interacting proteins with interactions of different confidence levels.
Fig. S10. Fractions of functionally similar pairs for interacting proteins with interactions of different confidence levels.
Fig. S11. Interactions in the fission and budding yeast MAPK pathways.
Fig. S12. Sensitivity assays for deletion strains of *S. pombe* KGY553 (ATCC) under various stress conditions (n = 3 experiments).
Table S1. Interactome sizes.
Table S2. *S. pombe* ORFs screened.
Table S3. StressNet and interaction confidence scores.
Table S4. Positive reference set.
Table S5. Random reference set.
Table S6. StressNet genes and number of interactions.
Table S7. StressNet—Conservation and rewiring.
Table S8. Primers used.

REFERENCES AND NOTES

1. H. Yu, P. Braun, M. A. Yildirim, I. Lemmens, K. Venkatesan, J. Sahalie, T. Hirozane-Kishikawa, F. Gebreab, N. Li, N. Simonis, T. Hao, J. F. Rual, A. Dricot, A. Vazquez, R. R. Murray, C. Simon, L. Tardivo, S. Tam, N. Svrzikapa, C. Fan, A. S. de Smet, A. Motyl, M. E. Hudson, J. Park, X. Xin, M. E. Cusick, T. Moore, C. Boone, M. Snyder, F. P. Roth, A. L. Barabási, J. Tavernier, D. E. Hill, M. Vidal, High-quality binary protein interaction map of the yeast interactome network. *Science* **322**, 104–110 (2008).
2. T. Ito, T. Chiba, R. Ozawa, M. Yoshida, M. Hattori, Y. Sakaki, A comprehensive two-hybrid analysis to explore the yeast protein interactome. *Proc. Natl. Acad. Sci. U.S.A.* **98**, 4569–4574 (2001).
3. P. Uetz, L. Giot, G. Cagney, T. A. Mansfield, R. S. Judson, J. R. Knight, D. Lockshon, V. Narayan, M. Srinivasan, P. Pochart, A. Qureshi-Emili, Y. Li, B. Godwin, D. Conover, T. Kalbfleisch, G. Vijayadamodar, M. Yang, M. Johnston, S. Fields, J. M. Rothberg, A comprehensive analysis of protein-protein interactions in *Saccharomyces cerevisiae*. *Nature* **403**, 623–627 (2000).
4. E. Formstecher, S. Aresta, V. Collura, A. Hamburger, A. Meil, A. Trehin, C. Reverdy, V. Betin, S. Maire, C. Brun, B. Jacq, M. Arpin, Y. Bellaiche, S. Bellusci, P. Benaroch, M. Bornens, R. Chanet, P. Chavrier, O. Delattre, V. Doye, R. Fehon, G. Faye, T. Galli, J. A. Girault, B. Goud, J. de Gunzburg, L. Johannes, M. P. Junier, V. Mirouse, A. Mukherjee, D. Papadopoulo, F. Perez, A. Plessis, C. Rossé, S. Saule, D. Stoppa-Lyonnet, A. Vincent, M. White, P. Legrain, J. Wojcik, J. Camonis, L. Daviet, Protein interaction mapping: A *Drosophila* case study. *Genome Res.* **15**, 376–384 (2005).
5. L. Giot, J. S. Bader, C. Brouwer, A. Chaudhuri, B. Kuang, Y. Li, Y. L. Hao, C. E. Ooi, B. Godwin, E. Vitols, G. Vijayadamodar, P. Pochart, H. Machineni, M. Welsh, Y. Kong, B. Zerhusen, R. Malcolm, Z. Varrone, A. Collis, M. Minto, S. Burgess, L. McDaniel, E. Stimpson, F. Spriggs, J. Williams, K. Neurath, N. Ioime, M. Agee, E. Voss, K. Furtak, R. Renzulli, N. Aanensen, S. Carrolla, E. Bickelhaupt, Y. Lazovatsky, A. DaSilva, J. Zhong, C. A. Stanyon, R. L. Finley Jr., K. P. White, M. Braverman, T. Jarvie, S. Gold, M. Leach, J. Knight, R. A. Shimkets, M. P. McKenna, J. Chant, J. M. Rothberg, A protein interaction map of *Drosophila melanogaster*. *Science* **302**, 1727–1736 (2003).
6. N. Simonis, J. F. Rual, A. R. Carvunis, M. Tasan, I. Lemmens, T. Hirozane-Kishikawa, T. Hao, J. M. Sahalie, K. Venkatesan, F. Gebreab, S. Cevik, N. Klitgord, C. Fan, P. Braun, N. Li, N. Ayivi-Guedehoussou, E. Dann, N. Bertin, D. Szeto, A. Dricot, M. A. Yildirim, C. Lin, A. S. de Smet, H. L. Kao, C. Simon, A. Smolyar, J. S. Ahn, M. Tewari, M. Boxem, S. Milstein, H. Yu, M. Dreze, J. Vandenhaute, K. C. Gunsalus, M. E. Cusick, D. E. Hill, J. Tavernier, F. P. Roth, M. Vidal, Empirically controlled mapping of the *Caenorhabditis elegans* protein-protein interactome network. *Nat. Methods* **6**, 47–54 (2009).
7. S. Li, C. M. Armstrong, N. Bertin, H. Ge, S. Milstein, M. Boxem, P. O. Vidalain, J. D. Han, A. Chesneau, T. Hao, D. S. Goldberg, N. Li, M. Martinez, J. F. Rual, P. Lamesch, L. Xu, M. Tewari, S. L. Wong, L. V. Zhang, G. F. Berriz, L. Jacotot, P. Vaglio, J. Reboul, T. Hirozane-Kishikawa, Q. Li, H. W. Gabel, A. Elewa, B. Baumgartner, D. J. Rose, H. Yu, S. Bosak, R. Sequerra, A. Fraser, S. E. Mango, W. M. Saxton, S. Strome, S. Van Den Heuvel, F. Piano, J. Vandenhaute, C. Sardet, M. Gerstein, L. Doucette-Stamm, K. C. Gunsalus, J. W. Harper, M. E. Cusick, F. P. Roth, D. E. Hill, M. Vidal, A map of the interactome network of the metazoan *C. elegans*. *Science* **303**, 540–543 (2004).
8. Arabidopsis Interactome Mapping Consortium, Evidence for network evolution in an *Arabidopsis* interactome map. *Science* **333**, 601–607 (2011).

9. J. F. Rual, K. Venkatesan, T. Hao, T. Hirozane-Kishikawa, A. Dricot, N. Li, G. F. Berriz, F. D. Gibbons, M. Dreze, N. Ayivi-Guedehoussou, N. Klitgord, C. Simon, M. Boxem, S. Milstein, J. Rosenberg, D. S. Goldberg, L. V. Zhang, S. L. Wong, G. Franklin, S. Li, J. S. Albala, J. Lim, C. Fraughton, E. Llamosas, S. Cevik, C. Bex, P. Lamesch, R. S. Sikorski, J. Vandenhaute, H. Y. Zoghbi, A. Smolyar, S. Bosak, R. Sequerra, L. Doucette-Stamm, M. E. Cusick, D. E. Hill, F. P. Roth, M. Vidal, Towards a proteome-scale map of the human protein-protein interaction network. *Nature* **437**, 1173–1178 (2005).
10. U. Stelzl, U. Worm, M. Lalowski, C. Haenig, F. H. Brembeck, H. Goehler, M. Stroedicke, M. Zenkner, A. Schoenherr, S. Koeppen, J. Timm, S. Mintzlaff, C. Abraham, N. Bock, S. Kietzmann, A. Goedde, E. Toksoz, A. Droege, S. Krobitsch, B. Korn, W. Birchmeier, H. Lehrach, E. E. Wanker, A human protein-protein interaction network: A resource for annotating the proteome. *Cell* **122**, 957–968 (2005).
11. M. Sipiczki, Where does fission yeast sit on the tree of life? *Genome Biol.* **1**, REVIEWS1011 (2000).
12. V. Wood, R. Gwilliam, M. A. Rajandream, M. Lyne, R. Lyne, A. Stewart, J. Sgouros, N. Peat, J. Hayles, S. Baker, D. Basham, S. Bowman, K. Brooks, D. Brown, S. Brown, T. Chillingworth, C. Churcher, M. Collins, R. Connor, A. Cronin, P. Davis, T. Feltwell, A. Fraser, S. Gentles, A. Goble, N. Hamlin, D. Harris, J. Hidalgo, G. Hodgson, S. Holroyd, T. Hornsby, S. Howarth, E. J. Huckle, S. Hunt, K. Jagels, K. James, L. Jones, M. Jones, S. Leather, S. McDonald, J. McLean, P. Mooney, S. Moule, K. Mungall, L. Murphy, D. Niblett, C. Odell, K. Oliver, S. O'Neil, D. Pearson, M. A. Quail, E. Rabbinowitsch, K. Rutherford, S. Rutter, D. Saunders, K. Seeger, S. Sharp, J. Skelton, M. Simmonds, R. Squares, S. Squares, K. Stevens, K. Taylor, R. G. Taylor, A. Tivey, S. Walsh, T. Warren, S. Whitehead, J. Woodward, G. Volckaert, R. Aert, J. Robben, B. Grymonprez, I. Weltjens, E. Vanstreels, M. Rieger, M. Schäfer, S. Müller-Auer, C. Gabel, M. Fuchs, A. Düsterhöft, C. Fritzc, E. Holzer, D. Moestl, H. Hilbert, K. Borzym, I. Langer, A. Beck, H. Lehrach, R. Reinhardt, T. M. Pohl, P. Eger, W. Zimmermann, H. Wedler, R. Wambutt, B. Purnelle, A. Goffeau, E. Cadieu, S. Dréano, S. Gloux, V. Lelaure, S. Mottier, F. Galibert, S. J. Aves, Z. Xiang, C. Hunt, K. Moore, S. M. Hurst, M. Lucas, M. Rochet, C. Gaillardin, V. A. Tallada, A. Garzon, G. Thode, R. R. Daga, L. Cruzado, J. Jimenez, M. Sánchez, F. del Rey, J. Benito, A. Domínguez, J. L. Revuelta, S. Moreno, J. Armstrong, S. L. Forsburg, L. Cerutti, T. Lowe, W. R. McCombie, I. Paulsen, J. Potashkin, G. V. Shpakovski, D. Ussery, B. G. Barrell, P. Nurse, The genome sequence of *Schizosaccharomyces pombe*. *Nature* **415**, 871–880 (2002).
13. T. K. Gandhi, J. Zhong, S. Mathivanan, L. Karthick, K. N. Chandrika, S. S. Mohan, S. Sharma, S. Pinkert, S. Nagaraju, B. Periaswamy, G. Mishra, K. Nandakumar, B. Shen, N. Deshpande, R. Nayak, M. Sarker, J. D. Boeke, G. Parmigiani, J. Schultz, J. S. Bader, A. Pandey, Analysis of the human protein interactome and comparison with yeast, worm and fly interaction datasets. *Nat. Genet.* **38**, 285–293 (2006).
14. A. Roguev, S. Bandyopadhyay, M. Zofall, K. Zhang, T. Fischer, S. R. Collins, H. Qu, M. Shales, H. O. Park, J. Hayles, K. L. Hoe, D. U. Kim, T. Ideker, S. I. Grewal, J. S. Weissman, N. J. Krogan, Conservation and rewiring of functional modules revealed by an epistasis map in fission yeast. *Science* **322**, 405–410 (2008).
15. A. Shevchenko, A. Roguev, D. Schaft, L. Buchanan, B. Habermann, C. Sakalar, H. Thomas, N. J. Krogan, A. Shevchenko, A. F. Stewart, Chromatin Central: Towards the comparative proteome by accurate mapping of the yeast proteomic environment. *Genome Biol.* **9**, R167 (2008).
16. C. Stark, B. J. Breitkreutz, A. Chatr-Aryamontri, L. Boucher, R. Oughtred, M. S. Livstone, J. Nixon, K. Van Auken, X. Wang, X. Shi, T. Reguly, J. M. Rust, A. Winter, K. Dolinski, M. Tyers, The BioGRID Interaction Database: 2011 update. *Nucleic Acids Res.* **39**, D698–D704 (2011).
17. L. Salwinski, C. S. Miller, A. J. Smith, F. K. Pettit, J. U. Bowie, D. Eisenberg, The Database of Interacting Proteins: 2004 update. *Nucleic Acids Res.* **32**, D449–D451 (2004).
18. S. Kerrien, B. Aranda, L. Breuza, A. Bridge, F. Broackes-Carter, C. Chen, M. Duesbury, M. Dumousseau, M. Feuermann, U. Hinz, C. Jandrasits, R. C. Jimenez, J. Khadake, U. Mahadevan, P. Masson, I. Pedruzzi, E. Pfeiffenberger, P. Porras, A. Raghunath, B. Roechert, S. Orchard, H. Hermjakob, The IntAct molecular interaction database in 2012. *Nucleic Acids Res.* **40**, D841–D846 (2012).
19. B. Turner, S. Razick, A. L. Turinsky, J. Vlasblom, E. K. Crowdy, E. Cho, K. Morrison, I. M. Donaldson, S. J. Wodak, iRefWeb: Interactive analysis of consolidated protein interaction data and their supporting evidence. *Database* **2010**, baq023 (2010).
20. A. Ceol, A. Chatr Aryamontri, L. Licata, D. Peluso, L. Briganti, L. Perfetto, L. Castagnoli, G. Cesareni, MINT, the molecular interaction database: 2009 update. *Nucleic Acids Res.* **38**, D532–D539 (2010).
21. H. W. Mewes, A. Ruepp, F. Theis, T. Rattei, M. Walter, D. Frishman, K. Suhre, M. Spannagl, K. F. Mayer, V. Stümpflen, A. Antonov, MIPS: Curated databases and comprehensive secondary data resources in 2010. *Nucleic Acids Res.* **39**, D220–D224 (2011).
22. Z. Hu, D. M. Ng, T. Yamada, C. Chen, S. Kawashima, J. Mellor, B. Linghu, M. Kanehisa, J. M. Stuart, C. DeLisi, VisANT 3.0: New modules for pathway visualization, editing, prediction and construction. *Nucleic Acids Res.* **35**, W625–W632 (2007).
23. M. E. Cusick, H. Yu, A. Smolyar, K. Venkatesan, A. R. Carvunis, N. Simonis, J. F. Rual, H. Borick, P. Braun, M. Dreze, J. Vandenhaute, M. Galli, J. Yazaki, D. E. Hill, J. R. Ecker, F. P. Roth, M. Vidal, Literature-curated protein interaction datasets. *Nat. Methods* **6**, 39–46 (2009).
24. J. Das, H. Yu, HINT: High-quality protein interactomes and their applications in understanding human disease. *BMC Syst. Biol.* **6**, 92 (2012).
25. M. Ashburner, C. A. Ball, J. A. Blake, D. Botstein, H. Butler, J. M. Cherry, A. P. Davis, K. Dolinski, S. S. Dwight, J. T. Eppig, M. A. Harris, D. P. Hill, L. Issel-Tarver, A. Kasarskis, S. Lewis, J. C. Matese, J. E. Richardson, M. Ringwald, G. M. Rubin, G. Sherlock, Gene Ontology: Tool for the unification of biology. The Gene Ontology Consortium. *Nat. Genet.* **25**, 25–29 (2000).
26. P. Braun, M. Tasan, M. Dreze, M. Barrios-Rodiles, I. Lemmens, H. Yu, J. M. Sahalie, R. R. Murray, L. Roncari, A. S. de Smet, K. Venkatesan, J. F. Rual, J. Vandenhaute, M. E. Cusick, T. Pawson, D. E. Hill, J. Tavernier, J. L. Wrana, F. P. Roth, M. Vidal, An experimentally derived confidence score for binary protein-protein interactions. *Nat. Methods* **6**, 91–97 (2009).
27. I. Remy, S. W. Michnick, A highly sensitive protein-protein interaction assay based on Gaussia luciferase. *Nat. Methods* **3**, 977–979 (2006).
28. N. Ramachandran, E. Hainsworth, B. Bhullar, S. Eisenstein, B. Rosen, A. Y. Lau, J. C. Walter, J. LaBaer, Self-assembling protein microarrays. *Science* **305**, 86–90 (2004).
29. A. L. Barabasi, R. Albert, Emergence of scaling in random networks. *Science* **286**, 509–512 (1999).
30. H. Jeong, B. Tombor, R. Albert, Z. N. Oltvai, A. L. Barabási, The large-scale organization of metabolic networks. *Nature* **407**, 651–654 (2000).
31. G. Rustici, J. Mata, K. Kivinen, P. Lió, C. J. Penkett, G. Burns, J. Hayles, A. Brazma, P. Nurse, J. Bähler, Periodic gene expression program of the fission yeast cell cycle. *Nat. Genet.* **36**, 809–817 (2004).
32. A. Matsuyama, R. Arai, Y. Yashiroda, A. Shirai, A. Kamata, S. Sekido, Y. Kobayashi, A. Hashimoto, M. Hamamoto, Y. Hiraoka, S. Horinouchi, M. Yoshida, ORFeome cloning and global analysis of protein localization in the fission yeast *Schizosaccharomyces pombe*. *Nat. Biotechnol.* **24**, 841–847 (2006).
33. H. Yu, N. M. Luscombe, H. X. Lu, X. Zhu, Y. Xia, J. D. Han, N. Bertin, S. Chung, M. Vidal, M. Gerstein, Annotation transfer between genomes: Protein-protein interologs and protein-DNA regulogs. *Genome Res.* **14**, 1107–1118 (2004).
34. L. R. Matthews, P. Vaglio, J. Reboul, H. Ge, B. P. Davis, J. Garrels, S. Vincent, M. Vidal, Identification of potential interaction networks using sequence-based searches for conserved protein-protein interactions or "interologs". *Genome Res.* **11**, 2120–2126 (2001).
35. C. Shou, N. Bhardwaj, H. Y. Lam, K. K. Yan, P. M. Kim, M. Snyder, M. B. Gerstein, Measuring the evolutionary rewiring of biological networks. *PLoS Comput. Biol.* **7**, e1001050 (2011).
36. A. Ben-Hur, W. S. Noble, Choosing negative examples for the prediction of protein-protein interactions. *BMC Bioinformatics* **7** (suppl. 1), S2 (2006).
37. W. K. Huh, J. V. Falvo, L. C. Gerke, A. S. Carroll, R. W. Howson, J. S. Weissman, E. K. O'Shea, Global analysis of protein localization in budding yeast. *Nature* **425**, 686–691 (2003).
38. A. E. Hirsh, H. B. Fraser, Protein dispensability and rate of evolution. *Nature* **411**, 1046–1049 (2001).
39. H. B. Fraser, A. E. Hirsh, L. M. Steinmetz, C. Scharfe, M. W. Feldman, Evolutionary rate in the protein interaction network. *Science* **296**, 750–752 (2002).
40. D. U. Kim, J. Hayles, D. Kim, V. Wood, H. O. Park, M. Won, H. S. Yoo, T. Duhig, M. Nam, G. Palmer, S. Han, L. Jeffery, S. T. Baek, H. Lee, Y. S. Shim, M. Lee, L. Kim, K. S. Heo, E. J. Noh, A. R. Lee, Y. J. Jang, K. S. Chung, S. J. Choi, J. Y. Park, Y. Park, H. M. Kim, S. K. Park, H. J. Park, E. J. Kang, H. B. Kim, H. S. Kang, H. M. Park, K. Kim, K. Song, K. B. Song, P. Nurse, K. L. Hoe, Analysis of a genome-wide set of gene deletions in the fission yeast *Schizosaccharomyces pombe*. *Nat. Biotechnol.* **28**, 617–623 (2010).
41. M. Nei, T. Gojobori, Simple methods for estimating the numbers of synonymous and nonsynonymous nucleotide substitutions. *Mol. Biol. Evol.* **3**, 418–426 (1986).
42. N. Rhind, Z. Chen, M. Yassour, D. A. Thompson, B. J. Haas, N. Habib, I. Wapinski, S. Roy, M. F. Lin, D. I. Heiman, S. K. Young, K. Furuya, Y. Guo, A. Pidoux, H. M. Chen, B. Robbertse, J. M. Goldberg, K. Aoki, E. H. Bayne, A. M. Berlin, C. A. Desjardins, E. Dobbs, L. Dukaj, L. Fan, M. G. FitzGerald, C. French, S. Gujja, K. Hansen, D. Keifenheim, J. Z. Levin, R. A. Mosher, C. A. Müller, J. Pfiffner, M. Priest, C. Russ, A. Smialowska, P. Swoboda, S. M. Sykes, M. Vaughn, S. Vengrova, R. Yoder, Q. Zeng, R. Allshire, D. Baulcombe, B. W. Birren, W. Brown, K. Ekwall, M. Kellis, J. Leatherwood, H. Levin, H. Margalit, R. Martienssen, C. A. Nieduszynski, J. W. Spatafora, N. Friedman, J. Z. Dalgaard, P. Baumann, H. Niki, A. Regev, C. Nusbaum, Comparative functional genomics of the fission yeasts. *Science* **332**, 930–936 (2011).
43. R. D. Finn, J. Mistry, J. Tate, P. Coggill, A. Heger, J. E. Pollington, O. L. Gavin, P. Gunasekaran, G. Ceric, K. Forslund, L. Holm, E. L. Sonnhammer, S. R. Eddy, A. Bateman, The Pfam protein families database. *Nucleic Acids Res.* **38**, D211–D222 (2010).
44. P. M. Kim, L. J. Lu, Y. Xia, M. B. Gerstein, Relating three-dimensional structures to protein networks provides evolutionary insights. *Science* **314**, 1938–1941 (2006).

45. X. Wang, X. Wei, B. Thijssen, J. Das, S. M. Lipkin, H. Yu, Three-dimensional reconstruction of protein networks provides insight into human genetic disease. *Nat. Biotechnol.* **30**, 159–164 (2012).
46. H. M. Berman, J. Westbrook, Z. Feng, G. Gilliland, T. N. Bhat, H. Weissig, I. N. Shindyalov, P. E. Bourne, The Protein Data Bank. *Nucleic Acids Res.* **28**, 235–242 (2000).
47. J. Espadaler, O. Romero-Isart, R. M. Jackson, B. Oliva, Prediction of protein-protein interactions using distant conservation of sequence patterns and structure relationships. *Bioinformatics* **21**, 3360–3368 (2005).
48. J. Das, J. Mohammed, H. Yu, Genome scale analysis of interaction dynamics reveals organization of biological networks. *Bioinformatics* **28**, 1873–1878 (2012).
49. J. Qian, M. Dolled-Filhart, J. Lin, H. Yu, M. Gerstein, Beyond synexpression relationships: Local clustering of time-shifted and inverted gene expression profiles identifies new, biologically relevant interactions. *J. Mol. Biol.* **314**, 1053–1066 (2001).
50. L. Hakes, S. C. Lovell, S. G. Oliver, D. L. Robertson, Specificity in protein interactions and its relationship with sequence diversity and coevolution. *Proc. Natl. Acad. Sci. U.S.A.* **104**, 7999–8004 (2007).
51. W. K. Kim, D. M. Bolser, J. H. Park, Large-scale co-evolution analysis of protein structural interlogues using the global protein structural interactome map (PSIMAP). *Bioinformatics* **20**, 1138–1150 (2004).
52. C. S. Goh, A. A. Bogan, M. Joachimiak, D. Walther, F. E. Cohen, Co-evolution of proteins with their interaction partners. *J. Mol. Biol.* **299**, 283–293 (2000).
53. A. P. Gasch, Comparative genomics of the environmental stress response in ascomycete fungi. *Yeast* **24**, 961–976 (2007).
54. K. Shiozaki, P. Russell, Conjugation, meiosis, and the osmotic stress response are regulated by Spc1 kinase through Atf1 transcription factor in fission yeast. *Genes Dev.* **10**, 2276–2288 (1996).
55. N. Bone, J. B. Millar, T. Toda, J. Armstrong, Regulated vacuole fusion and fission in *Schizosaccharomyces pombe*: An osmotic response dependent on MAP kinases. *Curr. Biol.* **8**, 135–144 (1998).
56. P. L. Kastritis, I. H. Moal, H. Hwang, Z. Weng, P. A. Bates, A. M. Bonvin, J. Janin, A structure-based benchmark for protein-protein binding affinity. *Protein Sci.* **20**, 482–491 (2011).
57. C. J. Ryan, A. Roguev, K. Patrick, J. Xu, H. Jahari, Z. Tong, P. Beltrao, M. Shales, H. Qu, S. R. Collins, J. I. Kliegman, L. Jiang, D. Kuo, E. Tosti, H. S. Kim, W. Edelmann, M. C. Keogh, D. Greene, C. Tang, P. Cunningham, K. M. Shokat, G. Cagney, J. P. Svensson, C. Guthrie, P. J. Espenshade, T. Ideker, N. J. Krogan, Hierarchical modularity and the evolution of genetic interactomes across species. *Mol. Cell* **46**, 691–704 (2012).
58. A. Frost, M. G. Elgort, O. Brandman, C. Ives, S. R. Collins, L. Miller-Vedam, J. Weibezahn, M. Y. Hein, I. Poser, M. Mann, A. A. Hyman, J. S. Weissman, Functional repurposing revealed by comparing *S. pombe* and *S. cerevisiae* genetic interactions. *Cell* **149**, 1339–1352 (2012).
59. H. Yu, L. Tardivo, S. Tam, E. Weiner, F. Gebreab, C. Fan, N. Svrzikapa, T. Hirozane-Kishikawa, E. Rietman, X. Yang, J. Sahalie, K. Salehi-Ashtiani, T. Hao, M. E. Cusick, D. E. Hill, F. P. Roth, P. Braun, M. Vidal, Next-generation sequencing to generate interactome datasets. *Nat. Methods* **8**, 478–480 (2011).
60. K. Venkatesan, J. F. Rual, A. Vazquez, U. Stelzl, I. Lemmens, T. Hirozane-Kishikawa, T. Hao, M. Zenkner, X. Xin, K. I. Goh, M. A. Yildirim, N. Simonis, K. Heinzmann, F. Gebreab, J. M. Sahalie, S. Cevik, C. Simon, A. S. de Smet, E. Dann, A. Smolyar, A. Vinayagam, H. Yu, D. Szeto, H. Borick, A. Dricot, N. Klitgord, R. R. Murray, C. Lin, M. Lalowski, J. Timm, K. Rau, C. Boone, P. Braun, M. E. Cusick, F. P. Roth, D. E. Hill, J. Tavernier, E. E. Wanker, A. L. Barabási, M. Vidal, An empirical framework for binary interactome mapping. *Nat. Methods* **6**, 83–90 (2009).
61. L. Breiman, Random forests. *Mach. Learn.* **45**, 5–32 (2001).
62. E. M. Kleinberg, An overtraining-resistant stochastic modeling method for pattern recognition. *Ann. Stat.* **24**, 2319–2349 (1996).
63. V. Wood, M. A. Harris, M. D. McDowall, K. Rutherford, B. W. Vaughan, D. M. Staines, M. Aslett, A. Lock, J. Bähler, P. J. Kersey, S. G. Oliver, PomBase: A comprehensive online resource for fission yeast. *Nucleic Acids Res.* **40**, D695–D699 (2012).
64. M. Kellis, B. W. Birren, E. S. Lander, Proof and evolutionary analysis of ancient genome duplication in the yeast *Saccharomyces cerevisiae*. *Nature* **428**, 617–624 (2004).
65. P. Rice, I. Longden, A. Bleasby, EMBOSS: The European Molecular Biology Open Software Suite. *Trends Genet.* **16**, 276–277 (2000).
66. S. B. Needleman, C. D. Wunsch, A general method applicable to the search for similarities in the amino acid sequence of two proteins. *J. Mol. Biol.* **48**, 443–453 (1970).
67. M. Vingron, M. S. Waterman, Sequence alignment and penalty choice. Review of concepts, case studies and implications. *J. Mol. Biol.* **235**, 1–12 (1994).
68. S. Henikoff, J. G. Henikoff, Amino acid substitution matrices from protein blocks. *Proc. Natl. Acad. Sci. U.S.A.* **89**, 10915–10919 (1992).
69. A. Stein, A. Céol, P. Aloy, 3did: Identification and classification of domain-based interactions of known three-dimensional structure. *Nucleic Acids Res.* **39**, D718–D723 (2011).
70. R. D. Finn, M. Marshall, A. Bateman, iPfam: Visualization of protein-protein interactions in PDB at domain and amino acid resolutions. *Bioinformatics* **21**, 410–412 (2005).
71. R. Jansen, H. Yu, D. Greenbaum, Y. Kluger, N. J. Krogan, S. Chung, A. Emili, M. Snyder, J. F. Greenblatt, M. Gerstein, A Bayesian networks approach for predicting protein-protein interactions from genomic data. *Science* **302**, 449–453 (2003).

Acknowledgments: We thank A. Bretscher for providing budding yeast deletion strains, S. Forsburg for providing fission yeast expression vectors, M. Smolka for experimental advice, and A. Clark and E. Alani for critical reading of our manuscript. **Funding:** J.D. was supported by the Tata Graduate Fellowship. A.M. was supported by Grant-in-Aid for Scientific Research (C). J.A.P. was supported by National Institute of General Medical Sciences (NIGMS) grant GM098634. F.P.R. was supported by NIH grant HG001715, by the Canada Excellence Research Chairs Program, and by the Canadian Institute for Advanced Research. This work was funded by NIGMS grant R01 GM097358 to H.Y. **Author contributions:** H.Y. and F.P.R. conceived the study. H.Y. designed all experiments and analyses and oversaw all aspects of the project. J.D. carried out upstream experimental design and all downstream computational analyses. A.M. and M.Y. were involved in Y2H library construction. T.V.V., V.T., A.G.D., L.W., and N.A.C. performed interactome screens using HT-Y2H. T.V.V. and N.A.C. performed PCR stitching. J.C.M. and F.P.R. performed Illumina sequencing. X. Wang performed sequence alignment for Stitch-seq. T.V.V. performed pairwise retests using HT-Y2H. H.Y. performed PCA and wNAPPA experiments. J.A.P. provided *S. pombe* strains. J.A.P., S.M.L., and H.Y. designed coimmunoprecipitation and stress response assays. X. Wei performed coimmunoprecipitation experiments. T.V.V. and N.K.-Z. performed stress response assays. J.D. and H.Y. wrote the manuscript with contributions from all authors. **Competing interests:** The authors declare that they have no competing interests. **Data and materials availability:** The Y2H data are available from HINT (http://hint.yulab.org), BioGRID (http://thebiogrid.org/), and IntAct (http://www.ebi.ac.uk/intact/).

Submitted 27 June 2012
Accepted 3 May 2013
Final Publication 21 May 2013
10.1126/scisignal.2003350
Citation: J. Das, T. V. Vo, X. Wei, J. C. Mellor, V. Tong, A. G. Degatano, X. Wang, L. Wang, N. A. Cordero, N. Kruer-Zerhusen, A. Matsuyama, J. A. Pleiss, S. M. Lipkin, M. Yoshida, F. P. Roth, H. Yu, Cross-species protein interactome mapping reveals species-specific wiring of stress response pathways. *Sci. Signal.* **6**, ra38 (2013).